MODELLING AND CLASSIFICATION OF HELICOPTER COMBAT MANOEUVRES

D.G. Thomson and R. Bradley
Department of Aerospace Engineering
University of Glasgow
Glasgow, G12 8QQ
Scotland

Abstract

There is an increasing number of flight mechanics studies where the influence of manoeuvre type has been found to be of importance, most notably the recent upgrade to the U.S. Mil. Spec. requirements. Another recent development has been the wider use of inverse simulation where a modelled flight path is used to drive a helicopter mathematical model in turn producing the control actions required to fly it. Although the influence of the manoeuvre on the performance of the helicopter has been established, there is little information on the actual form of the manoeuvre, or on how mathematical representations may be constructed. The aim of this paper has been to categorise the various types of manoeuvre commonly used in helicopter military operations, then develop algorithms capable of defining them mathematically. Several manoeuvres are fully modelled in the paper, and it becomes apparent that the techniques used may be applied to any number of different manoeuvres. By way of validation, data from flight tests has been used for comparisons with modelled flight paths and manoeuvre parameters. Methods of grading manoeuvres are also presented along with a discussion on the choice of suitable mathematical functions.

Nomenclature

C_T	Thrust coefficient
C_w	Weight coefficient
g	Acceleration due to gravity
h	Height above xy plane
k	Fraction of manoeuvre in entry and exit transients
m	Mass of helicopter
n_{fp}	Flight path load factor
n_p	Load factor normal to flight path
n_t	Load factor tangential to flight path
n_{Th}	Thrust factor
n_{θ_0}	Collective factor
R	Rotor radius
R_c	Radius of circular track
R_e	Radius of equivalent circular track
s	Distance around track
t	Time
T	Main rotor thrust
t_m	Manoeuvre time
V	Flight velocity
V_{max}	Maximum velocity attained
$\dot{V}$	Acceleration along flight path
x, y, z	Helicopter position in earth axes
$\dot{x}, \dot{y}, \dot{z}$	Component velocities in earth axes
$\ddot{x}, \ddot{y}, \ddot{z}$	Component accelerations in earth axes
x_e, y_e	Flight path co - ordinates at exit from turn
χ	Track angle
$\dot{\chi}$	Turn rate
χ_e	Track angle at exit from turn
$\dot{\chi}_m$	Maximum turn rate
γ	Flight path angle
θ_0	Main rotor collective pitch angle
$\theta_{0_{tr}}$	Tail rotor collective pitch angle
θ_{1_s}	Main rotor longitudinal cyclic pitch
θ_{1_c}	Main rotor lateral cyclic pitch
ρ	Density of air
Ω	Rotational speed of main rotor

1. Applications and Origins of Standard Manoeuvres for Helicopters

For all aircraft their performance in the execution of a variety of standard manoeuvres is a significant element of their assessment. Fixed wing aircraft, to take obvious examples, may have various aspects of their performance assessed with respect to :- take-off, landing, and turning and vertical loop. Rotorcraft have a versatility that has led to their use in a variety of applications each of which may possess its own characteristic manoeuvres. Take-off and landing are also, of course, necessary manoeuvres for rotorcraft, Figure 1, for example shows the take off requirements as specified by the Federal Aviation Authority, [1, 2]. Before a helicopter is certified airworthy, the manufacturer must show that the requirements specified by certifying body (the FAA in the United States, for example) can be met. In the case of the take-off manoeuvre shown in Figure 1, the manufacture must determine the normal take-off distance in a range of atmospheric conditions (temperature and altitude) and configurational conditions (centre of gravity position, one engine inoperative etc.) given that a height of 50ft. must be reached. To some extent, therefore, the certifying body has defined the shape of the manoeuvre. In the landing case, a certain amount of forward speed is desirable to avoid the vortex ring condition, while, in the take-off, safety considerations may require a certain angle of climb in order to maximise the chance of survival in the event of engine failure. This condition is shown in Figure 1 where safety regulations require the manufacturer to show that the helicopter can perform a safe landing should there be an engine failure at the Critical Decision Point (CDP) during take-off.

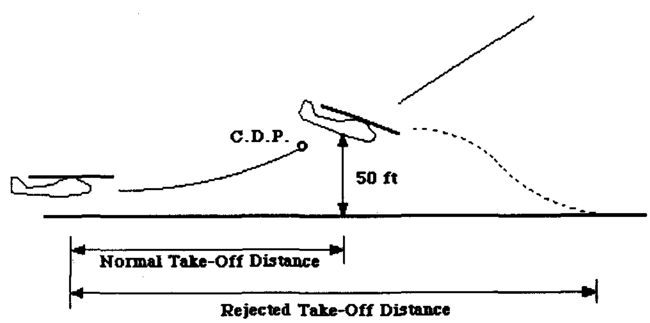

Figure 1 : FAA Take-off Regulations

In the military sphere of operation there has been considerable development in the battlefield helicopter where many standard manoeuvres are employed. The manoeuvres can be conveniently grouped into four headings :- obstacle avoidance, concealment, weapons aiming and delivery, and target acquisition and tracking. As examples of these we have, in Figure 2, the Pop-up manoeuvre to avoid an obstacle of a certain height by overflying it, followed by Figure 3 illustrating a Side-step which is a repositioning manoeuvre between areas of cover. Figure 4 then shows the Bob-up which is a vertical repositioning manoeuvre which is used for weapons delivery especially when the helicopter is equipped with a mast mounted sight. Finally, Figure 5 shows a ground target acquisition manoeuvre known as the Tear-drop Turn. The precision with which these manoeuvres are defined varies between applications. The recently published handling qualities specification [3] contains several manoeuvres, defined in terms of the required flight path, which must be achievable with Level 1 handling. The basic manoeuvres of the handling qualities document are Mission Task Elements (MTE's) and, as their name suggests, they are considered to be the building blocks of an operational mission as far as handling qualities are concerned - representing those parts of the mission where the quality of the helicopter handling is a key parameter. The Bob-up, Side-step and Pop-up (also known as the "Dolphin") are incorporated in the list of MTE's along with several others including the Quick-Hop, Figure 6, ("Rapid Acceleration and Deceleration").

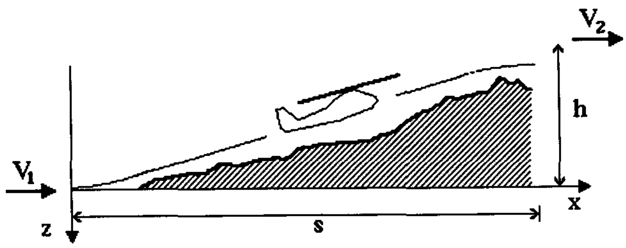

Figure 2 : The Pop-up Manoeuvre

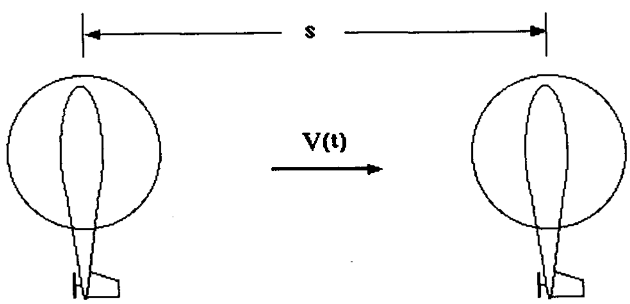

Figure 3 : The Side-step Manoeuvre

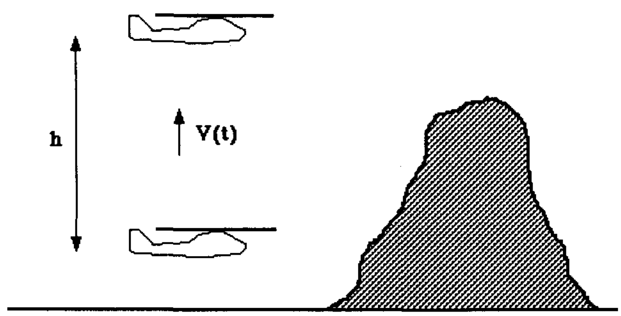

Figure 4 : The Bob-up Manoeuvre

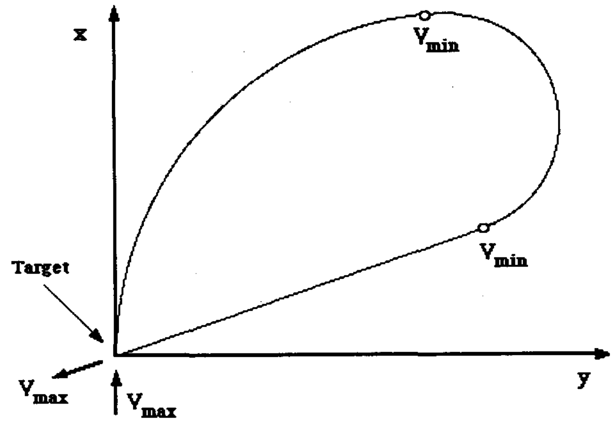

Figure 5 : The Tear-drop Turn Manoeuvre

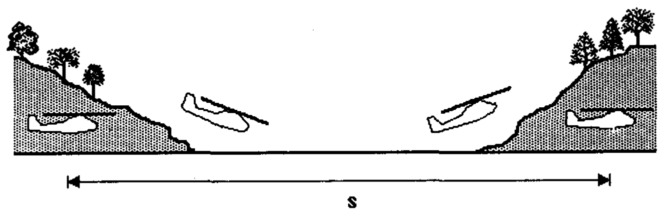

Figure 6 : The Quick-hop Manoeuvre

It is apparent that both the authors of the FAA regulations, and the Mil. Spec. Requirements have gone some way towards producing precise definitions of manoeuvres. In particular, several of the MTE's in Reference 3 are described in terms of flight path, attitude and velocity limits. Although this gives good insight into what the manoeuvre should look like, there has been no attempt to produce mathematical representations of them. Of course, the descriptions given by Hoh et al in Reference 3 are more than adequate for handling qualities flight test purposes, however there are two other important applications where a complete mathematical and/or numerical description is required : classification and grading of manoeuvres, and inverse simulation. This paper will focus on the modelling of helicopter manoeuvres for application to inverse simulation studies and for manoeuvre classification and grading. A study showing how manoeuvres may be classified is given, by necessity, in Section 5 after the manoeuvre defining techniques have been presented in Section 3, and validated in Section 4. At this stage, however, more insight into the requirements of manoeuvre-defining algorithms might be gained by first discussing exactly what is meant by inverse simulation.

2. Inverse Simulation

Inverse simulation can be defined as the computation of the control inputs to a dynamic system necessary to produce a desired output state. In the case of helicopter flight, the output state can be expressed in terms of a flight path, and the calculated inputs are, of course, the pilot's control displacements: main rotor collective, θ_0, longitudinal and lateral cyclic, θ_{1s}, θ_{1c}, and tail rotor collective, θ_{0tr}. This form of simulation is ideally suited to helicopter flight where, as demonstrated above, there are a large number of standard manoeuvres employed. A computer package capable of performing inverse simulations for helicopters, HELINV, has been developed at the University of Glasgow [4], and has been used for several flight mechanics studies [5, 6, 7]. One of the most recent applications [8] has been a study which has confirmed the validity of the inverse simulation algorithm, and also contributed towards the validation of the mathematical model used - the Royal Aerospace Establishment's (RAE) HELISTAB model [9]. A complete discussion of the inverse simulation algorithm would be inappropriate here, but full details are given by the authors of References 4 and 5. It is important, however, to detail the requirements that the manoeuvre defining algorithms must fulfil.

2.1 Requirements for Manoeuvre Defining Algorithms for Inverse Simulation

The basis of HELINV is the ability to calculate the control displacements required to produce a predefined unsteady flight condition. It is necessary that before the control angles are calculated, the rotor thrust, and its direction, must be found. This will require knowledge of the velocity and acceleration of the helicopter, from which the force and moment components (inertial, gravitational and aerodynamic) may be estimated. The first, and most basic requirement of the manoeuvre-defining algorithm is therefore that it must be able to compute the velocities and accelerations of the helicopter throughout the manoeuvre. As the simulation is in the form of a time response, it follows that the velocities and accelerations must be expressed as functions of time.

The only other major requirement of the manoeuvre-modelling algorithms is that the analytical functions defining flight path definitions must display a realistic degree of continuity. In the case of a helicopter inverse simulation, the flight path acts as the input to the system. It follows that if the input is discontinuous then it will act on the system in a way similar to a series of step inputs, and it has been shown [6] that the effect on the vehicle response can be unrepresentative. Lack of appropriate smoothness in the flight path is most likely to be observable in responses in regions of the flight path where curved and linear sections are joined.

A contributory part of the success of this package has been the modelling of this series of realistic Nap-of-the-Earth (NOE) manoeuvres, and the following section outlines the methodology used to produce the algorithms. Although the algorithms were created for use with HELINV, it will be shown in Section 5 that they can be used more generally for manoeuvre related studies.

3. Mathematical Modelling of Helicopter Combat Manoeuvres

It is often convenient in flight-mechanics modelling to set up earth fixed and body fixed origins and frames of reference. This allows the flight condition of the aircraft to be expressed in the earth axes frame, hence, independently from the dynamics of the vehicle. The velocities and accelerations expressed in earth axes can be transformed through the Euler angles, [10], Figure 7, to give their body fixed equivalents, and vice versa. Conventionally, the earth origin is located arbitrarily with the earth x-axis pointing northward, the y-axis eastward, and the z-axis pointing vertically downwards. In this paper, for convenience, the origin is positioned at the entry to the manoeuvre, and it is assumed that at the entry point, the helicopter's flight velocity vector is pointing in the earth x-axis direction. The position of the helicopter is taken to be the location, in the earth fixed frame, of the helicopter's centre of gravity. This is also normal practice as the body fixed origin is located at this point. To create a mathematical representation of a specific manoeuvre, the problem is then to express trajectory of the helicopter's centre of gravity position (x, y, z) within the earth axes system. If the flight velocity profile of the helicopter is also specified (preferably as a function of time) then it is possible to determine the components of earth axis velocities and

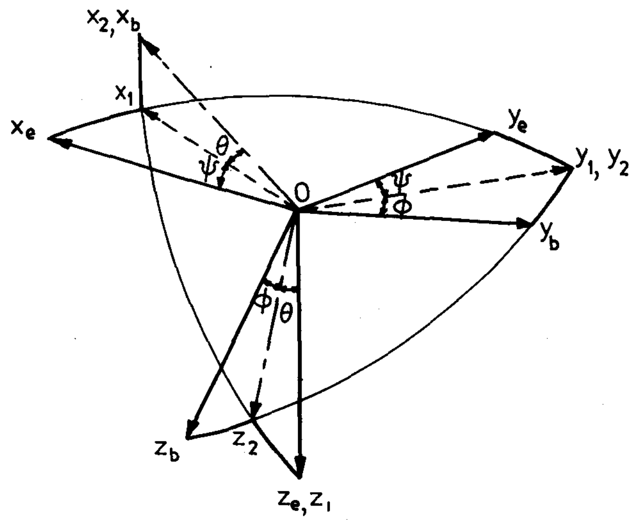

Figure 7 : Euler Angle Transformation Between Earth and Body Fixed Axes Systems

accelerations (as functions of time) through the whole manoeuvre. This is necessary as the earth axes velocities and accelerations may then be transformed to the body fixed frame, hence allowing the aerodynamic and inertial forces and moments of the vehicle to be calculated.

3.1 A General Flight Path Definition

Before modelling specific manoeuvres, it will be useful to introduce the basic theory by describing a general three dimensional manoeuvre such as the climbing turn shown in Figure 8(a). Figure 8(b) shows the manoeuvre track which is taken to be the projection of the flight path in the xy plane, and Figure 8(c) shows the altitude change around the manoeuvre. The angle between the velocity vector and the x direction in the x-y plane is known as the track angle, χ, and the angle between the s-axis and the velocity vector in the x-s plane is the angle of climb, γ. From Figure 8 it is apparent that the components of velocity in the earth fixed axes can be related to the flight velocity, V, and flight path angles χ, γ, by the expressions

$$\dot{x} = V \cos\gamma \cos\chi \tag{1}$$

$$\dot{y} = V \cos\gamma \sin\chi \tag{2}$$

$$\dot{z} = -V \sin\gamma \tag{3}$$

The component accelerations of the helicopter are then found by differentiation to be

$$\ddot{x} = \dot{V} \cos\gamma \cos\chi - V\dot{\gamma} \sin\gamma \cos\chi - V \dot{\chi} \cos\gamma \sin\chi \tag{4}$$

$$\ddot{y} = \dot{V} \cos\gamma \sin\chi - V\dot{\gamma} \sin\gamma \sin\chi + V \dot{\chi} \cos\gamma \cos\chi \tag{5}$$

$$\ddot{z} = -\dot{V} \sin\gamma - V\dot{\gamma} \cos\gamma \tag{6}$$

where

$\dot{V}$ = acceleration along flight path

$\dot{\gamma}$ = rate of change of flight path angle

$\dot{\chi}$ = turn rate

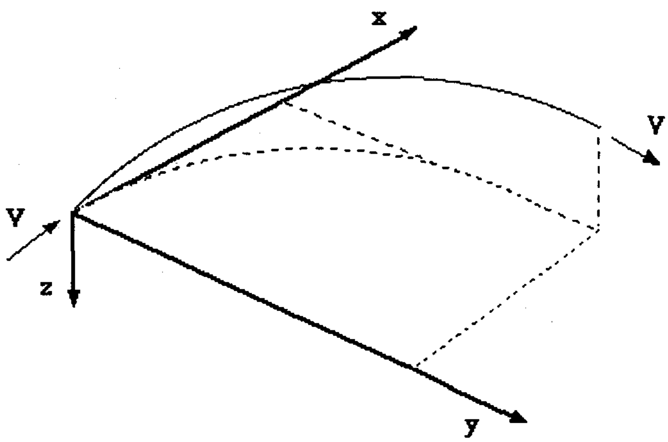

a) The 3-D manoeuvre

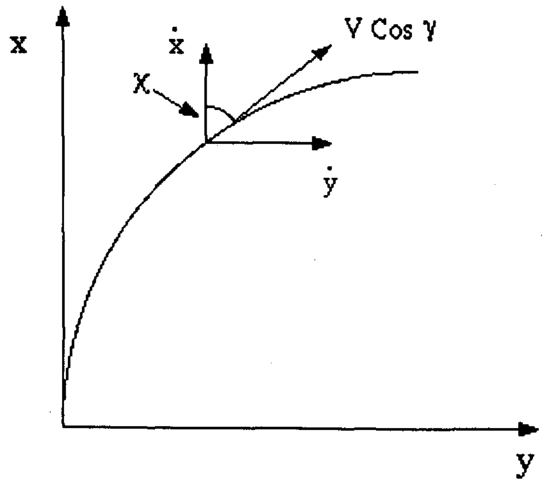

b) The Track

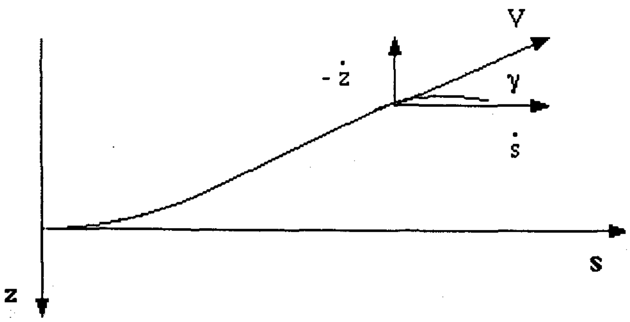

c) The Altitude

Figure 8 : A General 3-Dimensional Manoeuvre

If it was possible simply to write analytical expressions for x, y, and z as functions of time then, of course, equations 1 - 6 would not be required. This situation does not always arise, and, as will be demonstrated later, it is often easier to specify the flight velocity, the turn rate, and the altitude as functions of time, so that

$$\dot{\chi} = f_1(t) \tag{7}$$

$$z = f_2(t) \tag{8}$$

$$V = f_3(t) \tag{9}$$

By integrating equation (7) the track angle χ is found as a function of time. The z-axis velocity and acceleration can be found directly by differentiation of equation (8). Rearranging equation (3) gives

$$\gamma = -\sin^{-1}\left[\frac{\dot{z}}{V}\right] \tag{10}$$

and by differentiation

$$\dot{\gamma} = -\frac{\ddot{z}V - \dot{V}\dot{z}}{V^2 \cos\gamma} \tag{11}$$

As the velocity, V is also expressed as a function of time, equation (9), it is possible, using equations (1, 2, 4, 5), find the other component velocities and accelerations. Hence, any manoeuvre can be fully defined given the functions (7 - 9). The form these functions take depends on the geometry of the manoeuvre, as following examples will show.

3.2 The Pop-up Manoeuvre

As mentioned previously, the Pop-up manoeuvre, shown in Figure 2, is used for obstacle avoidance in NOE flight where the helicopter has to clear an obstacle of height, h, from a distance s. As described above, in order to develop a mathematical representation of this manoeuvre it is necessary to express turn rate, altitude and velocity as functions of time. Since the Pop-up manoeuvre is performed in the x-z plane (i.e. in two dimensions), there is no turn rate leaving only the flight velocity and altitude to define. It is important to consider the required flight path continuity before selecting the functions for altitude and flight velocity. It is not unreasonable to impose the condition that at the entry and the exit from the manoeuvre the helicopter should be in a level trimmed flight state. Considering first the flight velocity, this implies constant velocity at the entry to and exit from the manoeuvre ($V=V_1$ at $t=0$, and $V=V_2$ at $t=t_m$, say) and no acceleration at these points. Effectively, the velocity-defining function then has to satisfy four boundary conditions, and the simplest appropriate analytical function becomes a cubic polynomial, which can be shown to be of the form

$$V(t) = \left[-2\left(\frac{t}{t_m}\right)^3 + 3\left(\frac{t}{t_m}\right)^2\right](V_2 - V_1) + V_1 \tag{12}$$

The altitude function is similarly defined by considering the required conditions at entry and exit. The simplest set of boundary conditions are

$$\begin{aligned} &\text{i) } t = 0, \quad z = 0, \quad \dot{z} = 0, \quad \ddot{z} = 0 \\ &\text{ii) } t = t_m, \quad z = -h, \quad \dot{z} = 0, \quad \ddot{z} = 0 \end{aligned} \tag{13}$$

As well as giving the correct height change, setting the first derivative to zero ensures level flight, equation (10), and the trim state is ensured by setting the second derivative to zero. As there are six boundary conditions, a fifth order polynomial is the simplest suitable function, and the altitude-defining function is found to be

$$z(t) = \left[-6\left(\frac{t}{t_m}\right)^5 + 15\left(\frac{t}{t_m}\right)^4 - 10\left(\frac{t}{t_m}\right)^3\right]h \tag{14}$$

It is apparent from equations (12) and (14) that if the height, h, velocities, V_1 and V_2 and time t_m are specified, then the manoeuvre may be defined, however, it is much more convenient to specify the manoeuvre distance, s, the height and the velocities, then calculate the manoeuvre time. This is possible by first noting that

$$V = \sqrt{\dot{x}^2 + \dot{y}^2 + \dot{z}^2} \tag{15}$$

and, in the case of a Pop-up flown in the direction of the earth x-axis,

$$s = \int_0^{t_m} \sqrt{V^2 - \dot{z}^2}\ dt \tag{16}$$

This equation can be solved numerically to obtain the manoeuvre time t_m given s, h, V_1 and V_2. Other manoeuvres in the x-z plane can be defined in the same manner, indeed, the method of choosing boundary conditions then fitting a suitable polynomial can be adapted to suit other velocity, altitude or turn rate functions as will become apparent.

3.3 Linear Repositioning Manoeuvres

There are three linear repositioning manoeuvres commonly used in NOE flight : the Quick-Hop, Figure 6, the Side-Step, Figure 3, and the Bob-Up, Figure 4. In each case the helicopter begins and ends the manoeuvre in a trimmed hover flight state, translating over a specified linear distance in between. If it is assumed that the helicopter's body x-axis is in line with the earth x-axis, then the Quick-Hop manoeuvre is flown along the earth x-axis, the Side-Step manoeuvre is flown along the y-axis, and the Bob-up is flown along the z-axis. It is then apparent that the same definition may be used, with minor modifications, for each type of manoeuvre. As the manoeuvres are flown without deviation from a straight line there can be no turn rate, and the component velocity along the appropriate axis is simply equal to the flight velocity, so that

$$\begin{aligned} \text{Quick-Hop} &: \quad \dot{x}(t) = V(t) \\ \text{Side-Step} &: \quad \dot{y}(t) = V(t) \\ \text{Bob-Up} &: \quad \dot{z}(t) = V(t) \end{aligned} \tag{17}$$

To define the manoeuvre it is therefore sufficient to specify the flight velocity function, the first stage being to consider the boundary conditions which must be applied. As the manoeuvre is to begin and end in a trimmed hover flight state the four boundary conditions of zero velocity and acceleration at the entry and exit must be applied. During the manoeuvre the helicopter accelerates to some maximum velocity, V_{max}, then decelerates back to the hover. For convenience it is assumed that the maximum velocity is reached midway through the manoeuvre ($V=V_{max}$ at $t=t_m/2$). This condition and the four entry and exit conditions gives a fourth order polynomial as the simplest analytical function :

$$V(t) = \left[16\left(\frac{t}{t_m}\right)^4 - 32\left(\frac{t}{t_m}\right)^3 + 16\left(\frac{t}{t_m}\right)^2\right]V_{max} \tag{18}$$

As in the Pop-up, it is more convenient to specify the translational distance, s, over which the manoeuvre is to be performed rather than the time taken. Using this information to calculate the manoeuvre time by integrating the velocity gives :

$$t_m = \frac{15s}{8V_{max}} \tag{19}$$

Hence, by simply specifying a translational distance, s, and the maximum velocity to be achieved, V_{max}, it is possible to calculate the manoeuvre time, t_m from equation (19), then by integration of equation (18) the flight path co-ordinates can be found.

3.4 The Level Turn Manoeuvre

This example differs from the previous two in that here it is necessary to define a turn rate function. The most basic turn would simply consist of a circular arc which, noting that

$$\dot{\chi}(t) = \frac{V(t)}{R_c} \tag{20}$$

where R_c is the radius of the circular flight path, would give a constant turn rate assuming constant velocity. Using a circular arc poses the problem of continuity at the entry and exit sections of the manoeuvre where the circular flight path (with a finite value of turn rate) joins linear sections (with zero turn rate).

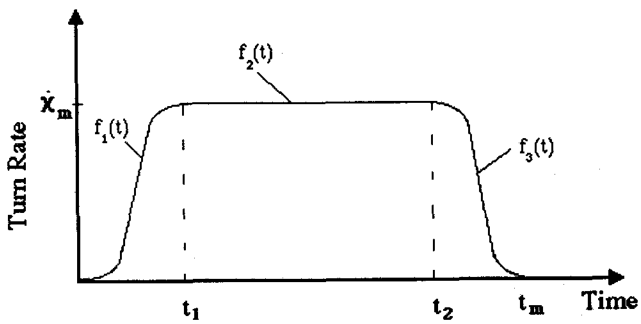

Figure 9 : Turn Rate in Level Turn Manoeuvre

This problem is overcome by imposing transient sections on the turn at the entry and exit points as shown in Figure 9, where the circular section and exit transients are reached after t_1 and t_2 seconds respectively. The resulting flight path is shown in Figure 10 where the broken line indicates the equivalent circular flight path of radius R_e, R_c is the radius of the circular section,

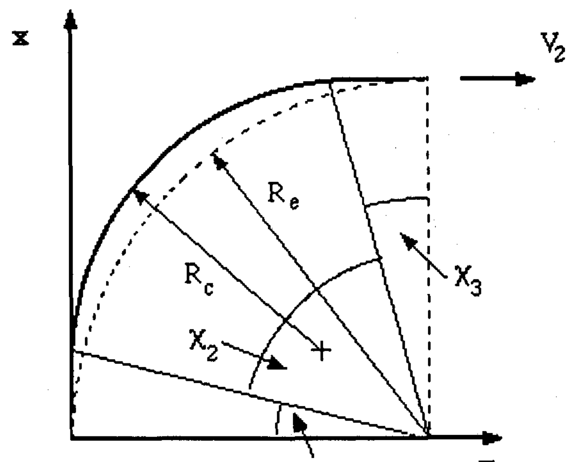

Figure 10 : The Level Turn Manoeuvre

χ_1, χ_2, and χ_3 are the track angles swept out in the entry transient, circular section, and exit transients respectively. It is convenient to define a parameter, k, which indicates the proportion of the manoeuvre spent in these transients, so that

$$\chi_1 = k\chi_e \qquad \chi_2 = (1-2k)\chi_e \qquad \chi_3 = k\chi_e \tag{21}$$

where χ_e is the track angle at the exit of the manoeuvre. The whole manoeuvre is assumed to be flown at a constant altitude (i.e. z(t) = constant), and as in the previous examples, it is assumed that the manoeuvre is initiated from a steady, level flight state. If a turn rate time history of the form given in Figure 9 is desired, then the manoeuvre must be performed at constant velocity, i.e. $V_1=V_2$, and this is the case which will be discussed here. The more general case which allows velocity to be varied through the manoeuvre is discussed in Reference 11. As both velocity and altitude are held constant, the manoeuvre may be defined simply by specifying an appropriate function for the turn rate. Referring to Figures 9 and 10, it is evident that there are three distinct sections in the manoeuvre (entry transient, circular arc, and exit transient), and it follows that the turn rate must be specified individually in each.

a) The Entry Transient

As in previous examples, the starting point is to consider the required conditions at the beginning and end of the section. As before, at the start of the manoeuvre a steady trim condition is required which gives a zero turn rate and acceleration condition at the entry to the manoeuvre. At time t_1 where the circular section is reached, the turn rate has increased to some maximum value dependent on the velocity V_c ($=V_1=V_2$) and radius of the circular section, R_c so that the boundary conditions, referring to Figure 9, are given by

$$\begin{aligned} &\text{i) } t=0,\quad \dot{\chi}=0,\quad \ddot{\chi}=0 \\ &\text{ii) } t=t_1,\quad \dot{\chi}=\frac{V_c}{R_c}=\dot{\chi}_m,\quad \ddot{\chi}=0 \end{aligned} \qquad (22)$$

A cubic polynomial is the simplest appropriate function, and applying these boundary conditions, it is found to be of the form

$$\dot{\chi}(t)=\left[-2\left(\frac{t}{t_m}\right)^3+3\left(\frac{t}{t_m}\right)^2\right]\dot{\chi}_m \qquad (23)$$

Noting that the track angle swept out in the transient can be found by integrating the turn rate over the time t_1,

$$\chi_1 = k\chi_e = \int_0^{t_1}\dot{\chi}(t)\ dt \qquad (24)$$

the time in the entry transient, t_1, is found to be

$$t_1 = \frac{2k\chi_e}{\dot{\chi}_m} \qquad (25)$$

b) The Circular Section

Turn rate is constant in this section, and, as in equation (24) by integration, the time t_2 is found to be

$$t_2 = t_1 + ((1-2k)\chi_e)/\dot{\chi}_m \qquad (26)$$

c) The Exit Transient

In this section the turn rate boundary conditions are defined as

$$\begin{aligned} &\text{i) } t=t_2,\quad \dot{\chi}=\dot{\chi}_m,\quad \ddot{\chi}=0 \\ &\text{ii) } t=t_m,\quad \dot{\chi}=0,\quad \ddot{\chi}=0 \end{aligned} \qquad (27)$$

This gives the required turn rate at the entry to the transient, and a straight line flight condition at the exit. As in the entry transient, a cubic polynomial is used to satisfy these conditions. The polynomial is of the form

$$\dot{\chi}(t)=\left[2t^3-3(t_m+t_2)t^2+6t_mt_2t-(3t_m-t_2)t_2^2\right]\left(\frac{\dot{\chi}_m}{(t_m-t_2)^3}\right)+\dot{\chi}_m \qquad (28)$$

Integration of this turn rate function between t_2 and the manoeuvre time t_m yields

$$t_m = t_2 + \frac{2k\chi_e}{\dot{\chi}_m} \qquad (29)$$

It is apparent that if the constant velocity, V_c, the transient fraction, k, the exit track angle, χ_e and radius of the circular section R_c were specified, then it would be possible to calculate all of the polynomial coefficients and times, hence the manoeuvre could be fully defined. This will not however, allow any control over the exit position. The most convenient way to specify the manoeuvre is by considering the equivalent circular path, Figure 10, and specifying the equivalent radius, R_e, hence ensuring that the required exit position is reached. An iterative scheme to calculate the circular arc radius, R_c, is required to achieve this: an initial guess of the value of R_c is made (based on the input value of R_e), the turn rate and component times through the manoeuvre are then calculated using equations (23-29), and by integrating equations (1) and (2) with $\gamma=0$, the exit co-ordinates are obtained.

$$\begin{aligned} x_e &= R_e\sin\chi_e = \int_0^{t_m} V(t)\cos\chi(t)\ dt \\ y_e &= R_e(1-\cos\chi_e) = \int_0^{t_m} V(t)\sin\chi(t)\ dt \end{aligned} \qquad (30)$$

From the above examples it is apparent that any manoeuvre may be specified by the use of simple polynomial expressions for the key parameters of altitude, turn rate and flight velocity. In the above examples the lowest suitable order of polynomial was always chosen to give the lowest suitable derivative continuity. Greater continuity can be achieved by increasing the order of the polynomial, and the effect this has on the manoeuvre profile is discussed in section 6. Before this is done, it is important to establish the validity of the mathematical representations. This may be achieved by comparing the modelled flight paths with data from flight tests.

4. Validation of Manoeuvres Against Flight Data

Validation is an important part of any modelling exercise. In this case, flight path data from agility flight trials has been used to validate the modelled trajectories by direct comparison. The flight trials were performed at the Royal Aerospace Establishment, Bedford, using a Westland Lynx helicopter and involved tests on a series of different manoeuvres. During the trials, the aircraft's states and controls are measured and recorded onboard, whilst its position relative to the ground is measured and recorded by a kinetheodolite tracking system. The positional co-ordinates are recorded at constant time intervals, and using numerical differentiation it is possible to determine the earth axis component velocities of the helicopter, and hence, using equation (15), the flight velocity can be determined. This information is now used to compare the flight paths from actual helicopter manoeuvres with those derived numerically in Section 3.

The first comparison made is of data measured in tests involving two linear repositioning manoeuvres: Side-step and Quick-hop [12]. In these trials, the pilot's objective was to fly the helicopter, from a hover condition, over a specified step length, then back to the hover again as aggressively as possible, whilst maintaining a constant height. This is equivalent to the definitions of the Quick-hop and Side-step discussed in Section 3.3. By examining the velocity profile from the flight trial the maximum velocity attained, V_{max}, was established and as the step size, s, is also known, there is enough information to produce a mathematical representation of the manoeuvre. In this case little information will be obtained by comparing flight paths as they are simply straight lines. Instead, as the linear repositioning manoeuvres are defined from their velocity profile, it is more appropriate to compare these. Figure 11 shows comparisons of the fourth order polynomial used to specify the flight velocity and the actual velocity from both Side-step (Fig. 11a) and Quick-hop (Fig. 11b) flight trials. In both cases it is apparent that the basic form of the helicopter's velocity profile is reproduced by the quartic function, however, there are small differences in the slope of the curve which will produce slightly different acceleration profiles. It is also noticeable that the assumption of maximum velocity at the mid point of the manoeuvre is valid.

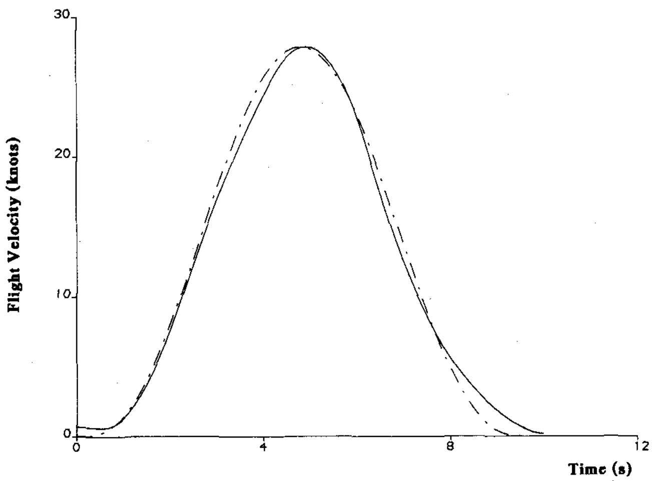

a) 200ft Side-step to the Right

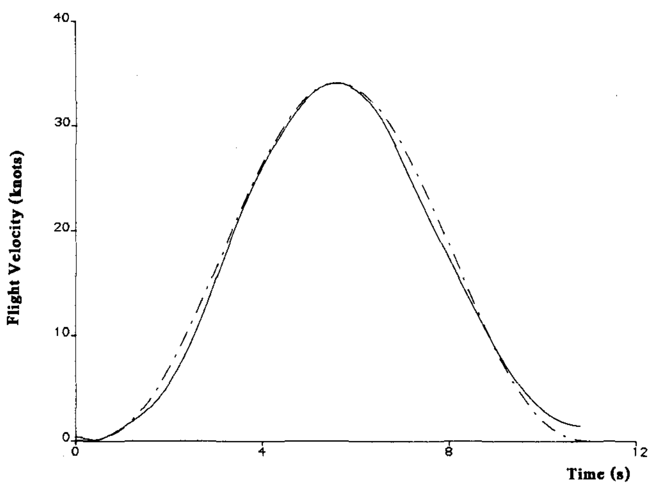

b) 300ft Quick-hop

FLIGHT DATA
4th ORDER POLYNOMIAL

Figure 11 : Comparison of Flight Velocity from Flight Data with that Modelled by a 4th Order Polynomial

The second set of data presented here was measured during trials aimed at studying the agility of helicopters in turning flight [13]. In these trials the pilots were instructed to perform turns of a specific radius by using markers on the ground for visual cues. The pilot was also instructed to maintain both a constant height and flight velocity through the manoeuvre. As with the linear repositioning manoeuvres this appears to be suitable for comparison with the turns defined in Section 3.4. Flight path data (positional co-ordinates) were obtained for a flight test where the pilot was instructed to fly a 400ft (122m) left hand turn at a constant velocity of 70 knots. From the data it was apparent that the pilot had actually flown a turn of radius 118m, shown as a series of triangular symbols on Figure 12. Thus the equivalent radius of the modelled turn, R_e is taken to be 118m, the exit track angle χ_e, is 90 degrees, and the constant flight velocity, V_c is 70 knots, leaving only the transient factor, k, to be determined. The most appropriate value of k is determined by varying it and comparing the resulting flight path with that measured in the flight trial. This is shown in Figure 12 where two modelled flight paths (k=0.1 and 0.2) are plotted alongside the measured flight path. It is clear that the value of 0.2 for k is the more suitable, indeed this gives a very good comparison between the actual and modelled flight paths.

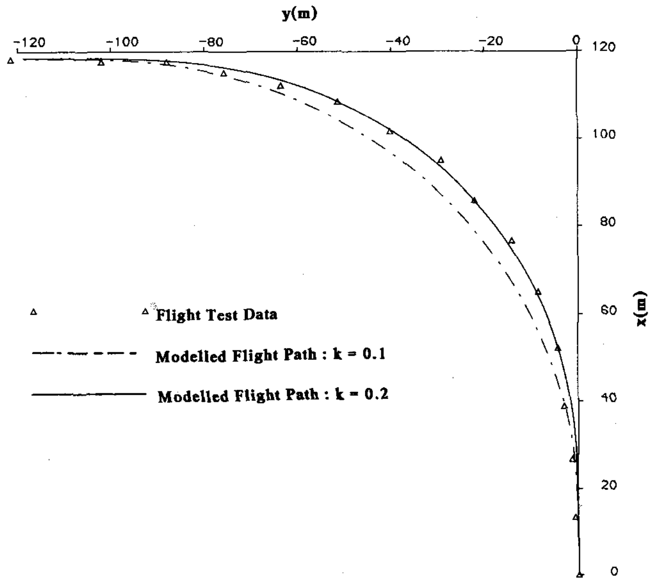

Figure 12 : Comparison of Track from Flight Trial with Modelled Flight Path

The examples shown here all suggest that the modelling techniques used give valid results. Without the availability of more flight data, particularly for height change manoeuvres such as the Pop-up, it is difficult to give a conclusive statement as to whether the techniques shown will be valid for all manoeuvres. The results so far are, however, encouraging.

5. Methods of Grading Manoeuvres

One result of a precise definition of a manoeuvre is that the ability of a helicopter to perform that manoeuvre can be assessed. This assessment can prove useful on three levels. Firstly, and the most basic consideration is whether the installed power can actually achieve the accelerations and decelerations of the helicopter inertia that the flight path requires. The second factor to be considered is whether the aerodynamic design of the helicopter will release that performance for use in executing the manoeuvre. Finally, an assessment of handling qualities will determine the ease with which the pilot can achieve the specified task. The first of these considerations can be approached simply from a definition of the flight path, and a simulation study incorporating a suitable model can supply the answers to the second. As yet the third consideration, that of handling qualities, is beyond the scope of non-piloted simulations and even stretches current flight simulator technology. In this section some criteria are introduced for grading manoeuvres in terms of severity. First this is done solely from flight path information and subsequently in combination with a helicopter simulation. No attempt is made to evaluate handling qualities as the simulations do not include a pilot.

5.1 Load Factors and Manoeuvre Severity Factor

The most common approach adopted when attempting to grade a manoeuvre is to examine the load factor. It is intended here to refer to a 'flight-path load-factor 'which is derived from the 'specific-force' of the manoeuvre, that is, the force per unit mass required to balance gravity and produce the flight path acceleration. This leads to the definition of the flight path load factor, n_{fp} according to

$$n_{fp} = \frac{1}{g}\sqrt{\left(\ddot{x}^2 + \ddot{y}^2 + (\ddot{z} - g)^2\right)} \tag{31}$$

It is also of interest to identify the two basic components of this force - the tangential component, n_t, for measuring the specific force along the flight path and the normal component, n_p associated with the curvature of the flight path

$$n_t = \frac{\dot{x}\ddot{x} + \dot{y}\ddot{y} + \dot{z}(\ddot{z} - g)}{g\sqrt{\dot{x}^2 + \dot{y}^2 + \dot{z}^2}} \tag{32}$$

$$n_p = \sqrt{n_{fp}^2 - n_t^2} \tag{33}$$

The three load factors for a Pop-up manoeuvre where the distance, s, to an obstacle of height, h, 25m, is 200m, flown with entry and exit velocities, V_1 and V_2 of 80 and 60 knots is given in Figure 13 plotted as a function of time. Having defined the flight path load factor we now have a simple basis for grading the severity of a manoeuvre. There are several ways to grade manoeuvres, two possibilities are shown here.

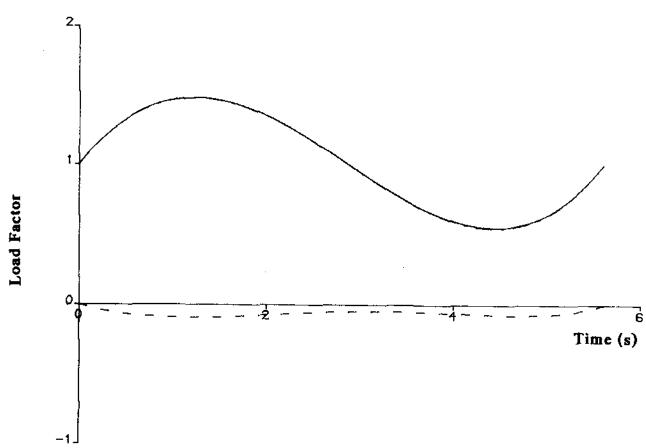

Figure 13 : Load Factors in a Pop-up Manoeuvre (s=200m, h=25m, V_1=80 knots, V_2=80 knots)

Firstly, the manoeuvre may be graded simply from the value of the maximum flight path load factor, n_{fpmax}, likely to be encountered. This is illustrated in Figure 14, where a n_{fpmax} values have been calculated for a series of similar Pop-up manoeuvres, where in each case the obstacle height was 25m, and the velocity was kept constant throughout the manoeuvre.

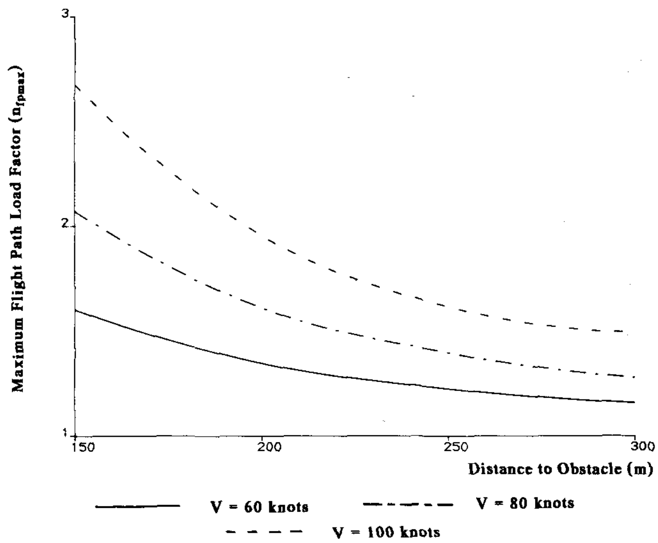

Figure 14 : Maximum Flight Path Load Factor in a Series of Pop-up Manoeuvres (h=25m)

Figure 14 shows the variation of n_{fpmax} against the distance to the obstacle for three constant velocities. The plots follow the expected form : low values of n_{fpmax} at the lower speeds and larger distances. The second possible method of grading manoeuvres involves integrating the flight path load factor over the duration of the manoeuvre. More specifically, a Manoeuvre Severity Factor (MSF) can be defined as

$$\text{M.S.F.} = \frac{1}{t_m}\int_0^{t_m} (n_{fp} - 1)^2\, dt \tag{34}$$

which represents the root mean square value of the departure of the flight path load factor from unity. Figure 15 shows the variation of MSF over the same series of manoeuvres as those in Figure 14. The same trend is evident : low speed longer distance manoeuvres being less severe. This second criteria, Manoeuvre Severity Factor, can be considered more suitable as it takes into account the possibility of sustained high load factors through the manoeuvre.

5.2 Thrust Factor

The introduction of a mathematical model of a helicopter enables the flight path to be used to drive an inverse simulation. The results of the simulation incorporate both aerodynamic effects and rotational inertias and their influence can be observed in the comparison of n_{fp} and the thrust factor, n_{Th}, which is defined as the ratio of thrust to weight coefficients.

$$n_{Th} = \frac{C_T}{C_w} \tag{35}$$

$$C_T = \frac{T}{\rho(\Omega R)^2 \pi R^2} \qquad C_w = \frac{mg}{\rho(\Omega R)^2 \pi R^2}$$

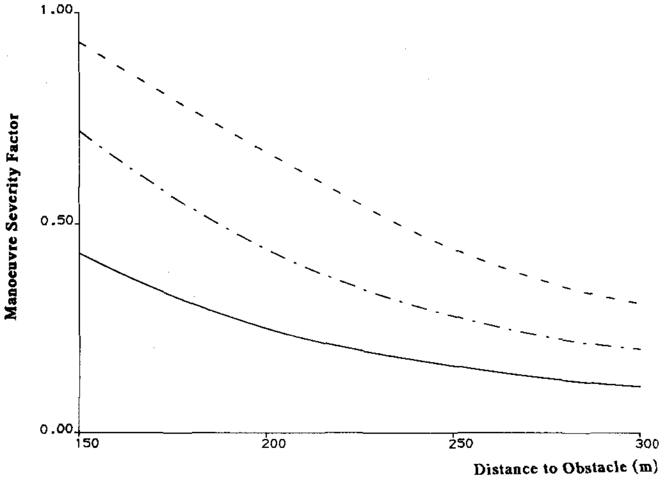

Figure 15 : Manoeuvre Severity Factor for a Series of Pop-up Manoeuvres (h=25m)

Figure 16 shows such a comparison for a Pop-up manoeuvre (s=200m, h=25m and V=80 knots, as in the example above) where the thrust factor throughout the manoeuvre has been calculated using a mathematical model of a Westland Lynx helicopter in the inverse simulation. At the entry and exit portions of the manoeuvre there is good correlation between the two plots. This is to be expected as in these regions the angle of attack of the helicopter fuselage is low, hence the aerodynamic forces and moments are also low. During the manoeuvre, as the angle of attack increases and the aerodynamic forces and moments become significant, there is a noticeable difference between the flight path load factor and the thrust factor. It is also possible to use maximum values of the thrust factor and measures of its departure from unity to quantify manoeuvre severity.

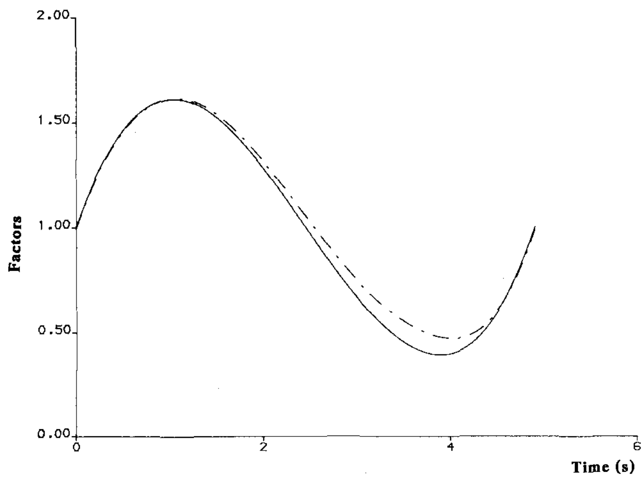

Figure 16 : Flight Path Load Factor and Thrust Factor for a Pop-up Manoeuvre (s=200m, h=25m, V=80 knots)

5.3 Collective Factor

The closest that this type of analysis can approach pilots' control actions is to generate control movements from the inverse simulation and attach suitable criteria to them. In the spirit of the discussion above, it is appropriate to relate the thrust factor to the collective displacement. Defining a collective factor, $n_{\theta 0}$ as

$$n_{\theta_0} = \frac{\theta_0}{\theta_{0_{trim}}} \tag{36}$$

where θ_{0trim} is the main rotor collective pitch angle at the trimmed entry to the manoeuvre, it is possible to compare the previously defined flight path load and thrust factors with one representing what the pilot actually has to do to fly the manoeuvre. In Figure 17 the same Pop-up manoeuvre can be used (s=200m, h=25m, V=80 knots), and data for a Westland Lynx helicopter was used in the inverse simulation. A major influence in the discrepancy is the inflow through the rotor and the collective ratio varies significantly from the thrust factor. Gradings of manoeuvre/helicopter combinations based on criteria attached to the collective ratio go some way to measuring the control movements demanded of the pilot by the particular helicopter configuration. Comparisons can be made for a single helicopter over a range of manoeuvres, or a variety of helicopter configurations over a series of manoeuvres.

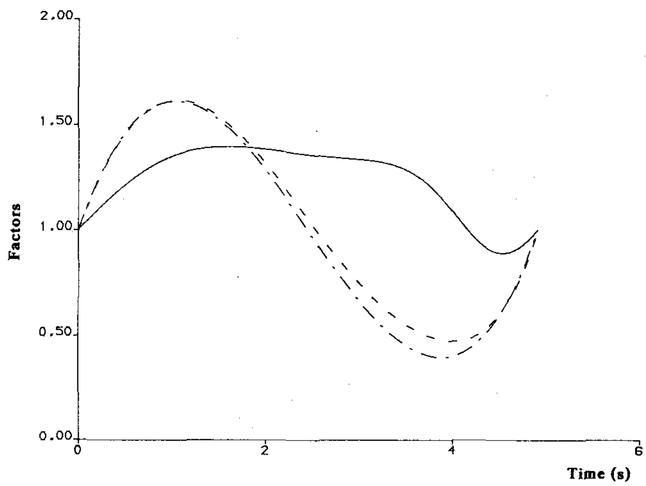

Figure 17 : Flight Path Load Factor, Collective Factor and Thrust Factor for a Pop-up Manoeuvre (s=200m, h=25m, V=80 knots)

6. The Effect of Polynomial Order on Manoeuvre

It is apparent from Section 3 that the methods used to create mathematical representations of helicopter flight paths rely to a large degree on the use of polynomial functions. As a general rule, the lowest order polynomial which gives a constant velocity and zero acceleration state at the entry and exit points was chosen. It is of course possible to choose polynomials of greater or lesser order, and the effect of doing so is discussed in this section.

The example taken is of the Pop-up manoeuvre. In Section 3.2 it was shown that a 5th order polynomial gave the required "trim" continuity at entry and exit for the Pop-up. If the zero acceleration requirement is neglected, two boundary conditions are lost, and a cubic polynomial is sufficient to define the manoeuvre. Another alternative is to apply the further conditions that the rate of acceleration (often referred to as "jerk") is required to be zero at entry and exit, the extra two boundary conditions giving a 7th order polynomial. The resulting flight paths are shown in Figure 18 along with the original 5th order polynomial trajectory. As the order of the

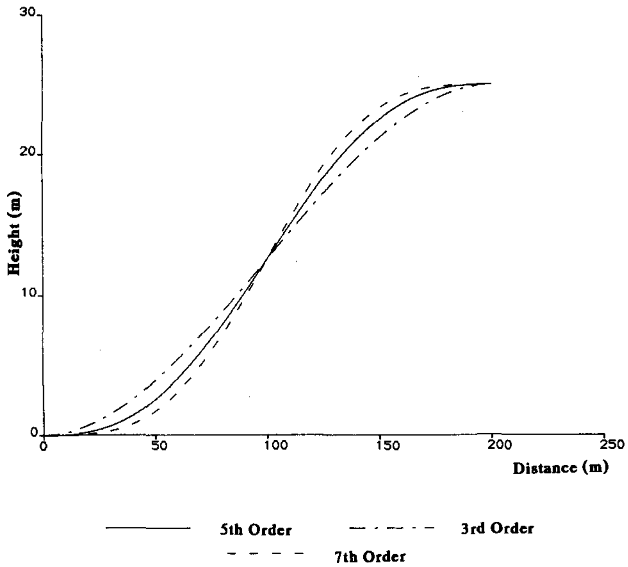

Figure 18 : Effect of Polynomial Order on Flight Path Shape for Pop-up Manoeuvre

polynomial is increased to produce higher order continuity at the entry and exit points, it is apparent that the flight path has become flatter at these regions. The flight path then has to have higher curvature in order to give the correct height change. The consequence this has on the maximum flight path load factor is shown in Figure 19. There are two points of interest concerning this plot. Firstly, the cubic polynomial flight path gives a linear load factor - this is because the second derivative of a cubic gives a constant slope. The other point of note is that as the order of the polynomial is increased the maximum flight path load factor also increases. In the above example a cubic polynomial was used to define the Pop-up, the result of this being discontinuities in acceleration at the entry and exits rendering this representation unsuitable. It is evident that whichever of the above criteria for grading the manoeuvres were applied to the higher order polynomial path, the result would be a higher severity factor.

In Section 4 comparisons were made between flight data and modelled flight paths. In each case good correlation was achieved using the minimum order polynomial for a trim state at entry and exit. In this section it is shown that other polynomials may also give these requirements but with important consequences on the severity of the manoeuvre. Without the benefit of flight data for the Pop-up manoeuvre it is impossible to say which order of polynomial gives the most accurate representation. However, in the light of the results from the validation exercise performed in Section 4, the use of the minimum order polynomial (in this case of order 5) in the first instance should give a good mathematical model of the flight path.

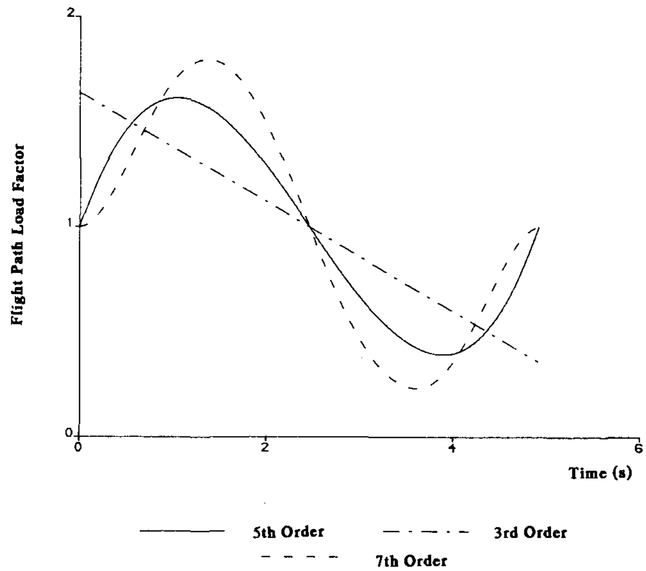

Figure 19 : Effect of Polynomial Order on Flight Path Load Factor for Pop-up Manoeuvre
(s=200m, h=25m, V=80 knots)

7. Conclusions

The following conclusions can be drawn from the research carried out in the field of manoeuvre modelling and classification presented in this paper.

1. A need for mathematical representations and classification of helicopter manoeuvres for use with inverse simulation packages, certification and handling qualities studies has been identified. Of these three applications, inverse simulation is the most demanding in terms of the required definition, a full numerical profile of the flight path being required. A less quantitative description may be required for the other applications which, at present, rely more on flight testing than simulation.

2. It has been shown that any manoeuvre can be defined by specifying the altitude, velocity and turn rate of the helicopter. The component velocities can be integrated to give the position of the helicopter.

3. The most convenient approach to adopt when modelling manoeuvres is to use simple polynomial curves to represent either the flight path itself or any of the vehicle velocities. Other functions such as trigonometric, for example, may also prove suitable.

4. There is good agreement between the assumed polynomial form and flight data for the manoeuvres where data is available.

5. Manoeuvres can be graded in terms of their severity. In order to do this a flight path load factor has been defined as being the specific force required to perform the manoeuvre. Further, by considering the variation of the flight path load factor through the manoeuvre it is possible to define a Manoeuvre Severity Factor. This gives a severity grading to a manoeuvre which is independent of the helicopter dynamics.

6. Having examined the effect of altering the order of the defining polynomial, it can be concluded that the most suitable polynomial is the lowest order one which gives the required entry and exit conditions.

Finally, a request should be made to those concerned with forming performance and handling qualities requirements. When manoeuvres are specified, the needs of simulation studies should be borne in mind. There is no need to go to the extent of defining precise trajectories, but there should be a complete statement of entry and exit conditions, and the conditions to be applied at significant internal parts of the manoeuvre. If this is done then the combination of manoeuvre modelling and inverse simulation can be a valuable design tool.

8. References

1. Federal Aviation Regulations, Part 29 - Airworthiness Standards : Transport Category Rotorcraft, 1974, U.S. Department of Transportation, Federal Aviation Administration.
2. Cerbe, T., Reichert, G. Optimisation of Helicopter Takeoff and Landing, Proceedings of the International Congress of the Aeronautical Sciences, 1988, Paper No. ICAS-88-6.1.2
3. Hoh, R.H., Mitchell, D.G., Aponso, B.L., Key, D.L., Blanken, C.L., Proposed Specification for Handling Qualities of Military Rotorcraft, Volume 1 - Requirements, USAAVSCOM Technical Report 87-A-4, May 1988.
4. Thomson, D.G., Bradley, R., Development and Verification of an Algorithm for Helicopter Inverse Simulation, Vertica, May 1990.
5. Thomson, D.G., Evaluation of Helicopter Agility Through Inverse Solution of the Equations of Motion, Ph.D. Dissertation, Department of Aeronautics and Fluid Mechanics, University of Glasgow, May 1987.
6. Thomson, D.G., Bradley, R. An Investigation of Flight Path Constrained Helicopter Manoeuvres by Inverse Simulation, Proceedings of the 13th European Rotorcraft Forum, Arles, France, September 1987.
7. Thomson, D.G., Bradley, R., An Investigation of Pilot Strategy in Helicopter Nap-of-the-Earth Manoeuvres by Comparison of Flight Data and Inverse Simulations, Proceedings of the Royal Aeronautical Society Conference: Helicopter Handling Qualities and Control, London, November 1988.
8. Bradley, R., Padfield, G.D., Murray-Smith, D.J., Thomson, D.G., Validation of Helicopter Mathematical Models, Transactions of the Institute of Measurement and Control.
9. Padfield, G.D., A Theoretical Model of Helicopter Flight Mechanics for Application to Piloted Simulation, RAE TR 81048, April 1981.
10. Etkin, B., Dynamics of Flight-Stability and Control, 2nd Edition, John Wiley, 1982
11. Thomson, D.G., Bradley, R. Mathematical Representation of Manoeuvres Commonly Found in Helicopter Nap-of-the-Earth Flight, Department of Aeronautics and Fluid Mechanics, University of Glasgow, Internal Report, Aero. Report 8801, Feb.1988.
12. Charlton, M.T., Padfield, G.D., Horton, Lt. Cdr, R.I., Helicopter Agility in Low Speed Manoeuvres, Paper 9.10, Proceedings of the 13th European Rotorcraft Forum Arles, France, September 1987.
13. Brotherhood, P., Charlton, M.T., An Assessment of Helicopter Turning Performance During Nap-of-the-Earth Flight, RAE Tech. Memo. FS(B) 534, January 1984

9. Acknowledgements

The authors wish to acknowledge the contribution of Dr G.D. Padfield of the Royal Aerospace Establishment, Bedford to this work, particularly in relation to the HELISTAB model and the flight data used in this study. This research was initially carried out as part of the Ministry of Defence Extra Mural Agreement 2048/39/XR/FS. Work is currently funded by the Royal Society under their 1983 Universities Research Fellowship scheme.